J Mater Sci (2011) 46:7247–7252
DOI 10.1007/s10853-011-5684-4

In situ high temperature X-ray diffraction study of UO_2 nanoparticles

R. Jovani Abril · R. Eloirdi · D. Bouëxière · R. Malmbeck · J. Spino

Received: 18 March 2011 / Accepted: 2 June 2011 / Published online: 17 June 2011

Abstract Nanocrystallites of UO_2 with a size of 3–5 nm were studied in situ with high temperature X-ray diffraction (HT-XRD), thermogravimetry (TGA), and differential thermal analysis. The evolution of the crystallite size, the lattice parameter, and the strain were determined from ambient temperature up to 1200 °C. Below 700 °C, a weak effect on the crystallite size occurs and it remains below 10 nm, while a strong expansion of the lattice parameter is measured. The strain decreases with temperature and is completely released at 700 °C. Above this temperature, begins the sintering of the nanocrystallites reaching a size of about 80 nm at 1200 °C. The weight loss curve observed in TGA is assigned to the desorption of water molecules and is correlated with the strain evolution observed by HT-XRD. The linear thermal expansion and the thermal expansion coefficient at 800 °C are 1.3% and 16.9×10^{-6} °C^{-1}, respectively.

Introduction

The continuous increasing interest in nanocrystalline materials [1–4] for most varied technological applications originates from the possibility to tune their magnetic, electronic, mechanic, and other properties, in such a way that their performance in comparison to standard materials can be remarkably superior. However, there is in general a critical size or critical grain size value above which the properties of nanocrystalline materials overlap with those of the bulk and therefore their advantage disappears. To follow and to describe the size-dependent property variations, the crystallite size, the lattice strain build up, and the lattice parameter evolution are key factors, which have to be considered and measured as precisely as possible. Transmission electron microscopy (TEM) techniques provide direct information on both size and shape of the nanoparticles and at the same time the structure of the single particles can be determined. However, the statistic evaluation of these parameters is in general time-consuming or not straightforward. X-ray diffraction provides the needed crystal-structure information and, through the use of the Hall–Williamson equation, also the average crystallite size and the strain created over the macroscopic sample volume can be provided. Abundant literature shows that the reduction in crystallite size is generally followed by variation of the lattice parameter [5–7]. The latter is directly related to the band structure and consequently to the physical properties modifications that occur as the dimension of the system diminishes.

The lattice parameter versus crystallite size response of the nanocrystalline systems has been widely studied and the results suggest that two antagonist behaviors can occur, showing either expansion or contraction of the lattice as the crystallite size decreases. On one side, lattice expansion at small crystallite size has been observed mainly for transition metal oxides as α-Fe_2O_3 [3], CeO_{2-x} [8], NiO [9], TiO_2 rutile [10], and MgO [11]. In contrast, lattice contraction with crystallite size is mainly assigned to metals or metalloid systems like Au, Pt [12, 13], Cu [14], Pd, Sn, and Bi [15]. However some exceptions to the rule exist and, thus for Ni, despite being a metal, lattice expansion for decreasing crystallite size [16] is observed, while for the oxide TiO_2 anatase [17], a typical metallic behavior is

R. J. Abril · R. Eloirdi (✉) · D. Bouëxière · R. Malmbeck · J. Spino
European Commission, Joint Research Centre, Institute for Transuranium Elements, Postfach 2340, 76125 Karlsruhe, Germany
e-mail: rachel.eloirdi@ec.europa.eu

displayed. Furthermore, for the same system and depending on the preparation method used, either lattice expansion or a lattice contraction with decreasing crystal size could be observed.

In the present study, UO_2 nanoparticles have been prepared by the hydrolysis route [18], in which an uranyl salt was dissolved in a NaCl solution, which was then electrolytically reduced (U^{6+} to U^{4+} conversion) and the nanoscale precipitation induced by slow addition of a NaOH solution (Jovani et al., private communication, 2010).

Use of bulk nanocrystalline UO_2 has been recently proposed for advanced nuclear fuels, for which enhanced mechanical behavior and superior fission gas retention capacity, in comparison to standard nuclear fuels, have been anticipated [19–21]. In this article, we report the high temperature X-ray diffraction (HT-XRD) study of UO_2 nanoparticles for nuclear fuel fabrication purposes. We analyze the effect of temperature on the crystallite size, which is a fundamental parameter in the sintering process. In addition, the variation of the lattice parameter versus crystal size and temperature, as well as data on the linear thermal expansion, are reported and compared to the bulk material.

Experimental

For the preparation of the UO_2 nanomaterial, the method described in literature [18] was employed and adjusted for high U-concentrations, as needed for production purposes. Details of the method will be reported in a further paper (Jovani et al., private communication, 2010). Nanoparticles of UO_2 were prepared by dissolving $UO_2(NO_3)_2$ in 1 M NaCl, followed by electrochemical reduction of U(VI) into U(IV) and by slow alkalinization of the mother solution with a 1 M NaOH solution. The formed precipitate was filtered in a centrifuge and then washed with deionised water to remove Na^+ and Cl^- species that were absorbed on the sample surface.

Differential thermal analyses (DTA) and thermogravimetry analysis (TGA) were employed under Ar-gas at a heating rate of 5 °C/min to determine the thermal decomposition temperature and the water content of the product. The apparatus used was a NETZSCH Simultaneous Analyzer STA 449 Jupiter. In situ HT-XRD patterns were acquired with a Bruker D8 powder diffractometer mounted in a Bragg–Brentano configuration, with a curved Ge monochromator (111), a Cu X-ray tube (40 kV, 40 mA), and a Position Sensitive detector Braun covering an angular range of 6° (2θ) and an Anton Paar HTK2000 heating chamber. Scans were collected from 20° to 120° in 2θ using 0.0146° step-intervals with counting steps of 2 s. The temperature range explored was 30–1200 °C; the working atmosphere was Helium. The unit cell parameter a of UO_2 was determined using $a = f(\cos^2\theta)$ function to correct the systematic peak shifts errors and to allow precise data acquisition [22]. The crystallite size and the mean strain e_0 in the material were determined by using the software Topas version 4.1 and used to characterize the microstructure and the deformation state of the material, respectively.

Results and discussion

The evolution with temperature of the UO_2 nanoparticles XRD pattern is shown in Fig. 1. The observed reflections are assigned to UO_2-fcc phase structure and to Pt-phase corresponding to the heater plate, plus an impurity peak at around $2\theta = 26°$. The pattern is similar to the one reported at room temperature by Rousseau et al. [18]. They reported the impurity peak as Na polyuranate, coming from precipitation of U(VI) with NaOH. The effect of temperature on the peaks can be better seen on the right-hand plot of Fig. 1, displaying the evolution of two main peaks of the UO_2 structure, the (111) and (200) reflections.

In Fig.1, one observes a shift in the peak position to lower angles, related to the lattice parameter expansion with increasing temperature. At room temperature, we determined a lattice parameter of about 0.545 nm, in agreement with literature [18]. A second effect of the temperature is seen in the width of the peaks which decreases with temperature while the intensity of the peaks increases. Since the contribution of instrumental broadening is independent of the temperature, the broadening is mainly related to the crystallite size and to the strain

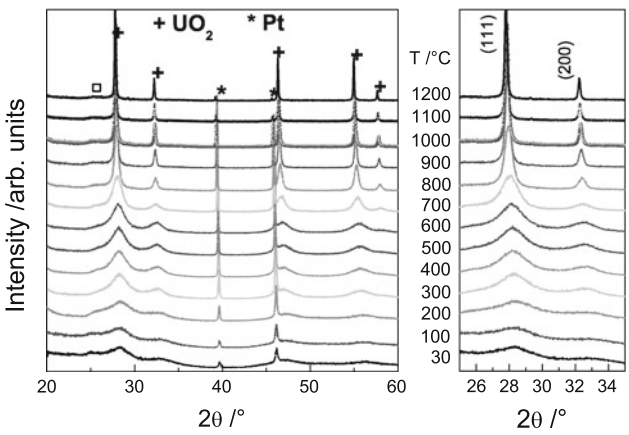

Fig. 1 *left* In-situ HT-XRD patterns of UO_2 nanoparticles. The patterns show *plus* peaks corresponding to UO_2, *asterisk* peaks for Pt heating plate, and a weak peak (*open square*) due to a residual impurity. *right* The evolution of (111) and (200) peaks of UO_2 cubic structure as a function of the temperature

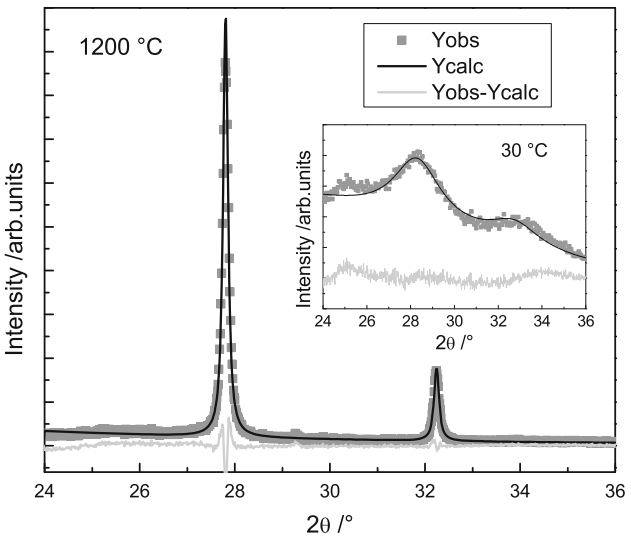

Fig. 2 Crystallite size and lattice strain/distortions were calculated using the software Topas based on the fundamental parameter approach. The full width at half maximum determination has been taken for the crystallite size curve. The diffraction patterns were refined using the fluorite crystalline structure (space group Fm-3m)

present in the material. The particle size was estimated from the width of the XRD lines. The software Topas enabled to determine both the crystallite size and the strain using the Hall–Williamson formula:

$$\beta = \frac{K\lambda}{D\cos\theta} + 4e_0 \tan\theta \quad (1)$$

where β is the full peak width at half maximum, K is a constant taken as 0.89 that depends upon the particle shape and the Miller-indexes (hkl), θ is the Bragg angle, λ is the wavelength of the radiation, D is the average particle size, and e_0 is the mean strain.

To refine the profile of the XRD patterns, a subroutine included in the program Topas version 4.1. was used. Using the fundamental parameter approach of the software, there was no need to perform measurements of a reference material to determine the contribution of the instrument to the peak broadening. Thus, only the instrument parameters had to be introduced in the program. A very good pattern refinement was obtained using a Pseudo-Voigt peak profile fitting function. Figure 2 displays examples of refinement performed on the pattern taken at 1200 °C and at ambient temperature (inset).

The crystallite size and the mean strain e_0 of the UO_2 nanoparticles obtained from Eq. 1 as a function of temperature are reported in Fig. 3. Here (and in Fig. 4) the marks A, B, and C are used to indicate the characteristic temperature of growth which are at 30, 300, and 700–800 °C respectively. At room temperature, the size of the crystallite was about 3–4 nm, which is in agreement with previous study [18] and with the particle size measured by TEM (Jovani et al., private communication, 2010). The crystallite size change with temperature shows two domains separated at 700 °C. Below that temperature, there was a weak influence on the crystallite size which evolved from 3 to 10 nm. Above 700 °C, the size of the crystallite increased quasi linearly but drastically with temperature, reaching a size of 80 nm at 1200 °C. The evolution of the mean strain e_0 can also be described within these temperature domains. However, at room temperature, the strain is at its maximum, it decreases completely to zero value at about 700 °C, where it is totally released. It is interesting to note that the complete release of the strain in the UO_2 nanoparticles coincides with the onset of the starting of the sintering of the crystallites. The decrease of the strain occurs in a two-step process, with an initial decrease of about 75% up to 300 °C. A second slower decrease occurs, reaching zero at 700 °C (Fig. 3). The strain present in the material can be related, a priori, to solvent molecules attached to the nanoparticles and to the related binding-strength. In this material, the solvent is mainly water.

In Fig. 4, the evolution of the lattice parameter versus the crystallite size and versus the temperature are shown. The main change in the lattice parameter occurs for crystal sizes below 10 nm. It increases steeply from 0.545 to 0.550 nm as the crystal size increases from 3 to 10 nm, while the temperature increases from 20 to 700 °C. Above 10 nm, a weak evolution of the lattice parameter with the crystallite size is observed. The evolution of the lattice parameter below 800 °C is not linear but follows a kind of power law. The values in this range fall below those of UO_2 and indicate a stoichiometry between $UO_{2.15}$ and $UO_{2.2}$, according to the data reported in literature for the bulk material [23]. Above 800 °C and thus above 10 nm, the lattice parameter versus temperature curve of the UO_2

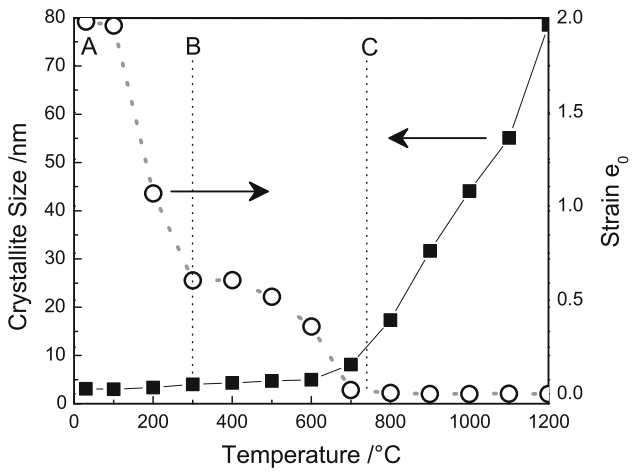

Fig. 3 Crystallite size versus temperature and mean strain versus the temperature in UO_2 nanoparticles

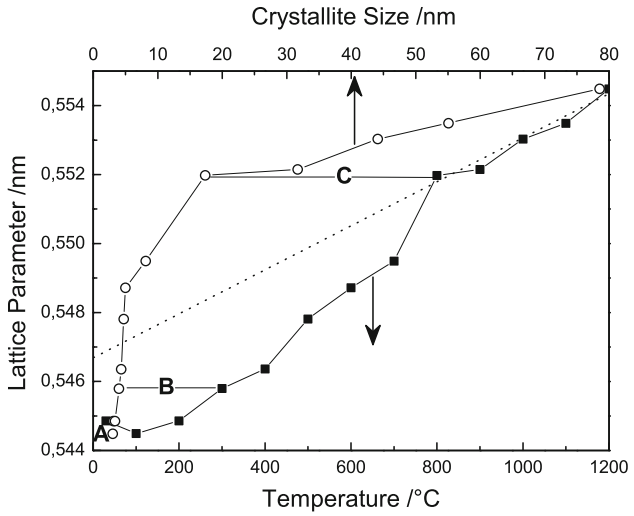

Fig. 4 Lattice parameter of UO_2 nanoparticle versus temperature and lattice parameter versus crystallite size

nanoparticles, whose linear trend is shown by the straight dotted line in the Fig. 4, is similar to that found for the UO_2 bulk.

From, the latter curve, the extrapolated value of the lattice parameter at 20 °C is 0.5468 nm, close to the one reported for UO_2 bulk at room temperature. It is well known that the lattice parameter of a non stoichiometric UO_{2+x} is linked to the oxygen content by the relation [24]:

$$a(\text{nm}) = 0.54705 - 0.0094x \quad (2)$$

Equation 2 is valid for values of x below 0.125 and extrapolation to higher x values may imply some uncertainty. Nevertheless, relating the lattice parameter found in our study to this formula, we found a stoichiometry of about $UO_{2.19}$, which is similar to the one reported by Rousseau et al. [18]. However, we remark that Eq. 2 and other equivalent relations are valid for bulk compounds; their applicability to nanoparticles may be still open to proof.

Rousseau et al. [18] reported a XPS data showing a contribution of U(VI) and U(IV) in the precipitated particles. Based on the lattice parameter determined by XRD, they concluded hence that the stoichiometry was $UO_{2.19}$, thus describing the system as UO_{2+x} nanoparticles.

Table 1 displays the linear thermal expansion (LTE) and the thermal expansion coefficient (LTEC) of UO_2 nanoparticles as a function of the temperature.

The LTE at temperature T were calculated by the relation :

$$\text{LTE} = \frac{(a_T - a_0) \times 100}{a_0} \quad (3)$$

where a_T is the lattice parameter at temperature T and a_0 is the lattice parameter at 20 °C.

The linear thermal expansion coefficient (LTEC) are calculated by differentiating the thermal expansion curve a_T versus T with respect to the temperature T:

$$\text{LTEC} = \frac{1}{a_0} \times \frac{\delta a_T}{\delta T} \quad (4)$$

The linear thermal expansion of the UO_2 nanoparticles for temperatures below 700 °C is smaller than for UO_2 bulk and for UO_{2+x} bulk [25] ($x = 0 - 0.13$ and $x = 0.23 - 0.25$). For comparison, values for the bulk are also supplied in Table 1. In contrast, for temperature above 800 °C, the trend is reversed and values are higher than those measured for UO_2 bulk. On the other hand, the LTEC is lower for UO_2 nanoparticles than for bulk UO_2 for temperatures below 800 °C. The LTEC in the nanoparticles tends to stabilize at high temperatures at a value of about $15 \times 10^{-6}\,°\text{C}^{-1}$, while

Table 1 Linear thermal expansion and LTEC of UO_2 nanoparticles and bulk

Temperature (°C)	Linear thermal expansion, % (bulk) [25]	Thermal expansion coefficient, $10^{-6} \times °\text{C}^{-1}$ (bulk) [25]
30	– (0.025)	– (9.74)
100	– (0.027)	– (9.74)
200	– (0.125)	– (9.8)
300	0.17234 (0.223)	6.38292 (9.99)
400	0.27622 (0.322)	7.46539 (10.12)
500	0.54253 (0.422)	11.54314 (10.27)
600	0.70899 (0.626)	12.43848 (10.51)
700	0.85087 (0.73)	12.69948 (10.78)
800	1.30695 (0.837)	16.97336 (11.12)
900	1.33778 (0.948)	15.37681 (11.53)
1000	1.49966 (1.062)	15.46041 (12.01)
1100	1.58445 (1.181)	14.80797 (12.56)
1200	1.76707 (1.305)	15.10316 (13.18)

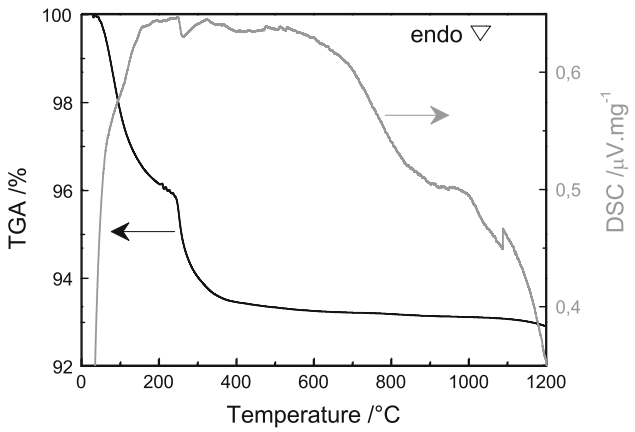

Fig. 5 TGA and DTA curves of UO_2 nanoparticle

for UO_2 bulk at 1200 °C LTEC is about 12×10^{-6} °C^{-1}. The thermal expansion coefficient in nanocrystalline materials is one of the physical properties linked to the nature of the nanocrystalline interfaces and depends mainly on anharmonic crystal lattice vibrations [26]. Basically, nanocrystalline materials are composed of two main parts, a crystal core and an interface. It is clearly demonstrated that the LTEC of nanocrystalline samples is enhanced relative to the coarse grained polycrystalline counterparts, due to the high density of interfaces or interfacial structures [27]. Theoretical calculations have shown also that the thermal expansion coefficient of the interface is associated with an interfacial excess volume [28]. This causes the property in the nanocrystalline material relative to the large crystalline state to increase on reducing its grain size. A previous study on the thermal expansion of Cu with small and large grain samples showed that the expansion coefficient of the former was 2–5 times larger than that of the copper single crystal, suggesting large anharmonic atomic vibrations in grain boundaries [29]. Also studies made on Nb films [30] and on nano-Fe [31] showed larger lattice expansion with reduction of the crystallite size. Nevertheless, a case exists where the lattice expansion is bigger in the bulk than in the nanoparticle state. Thus hexagonal Zn nanowires [32] with diameter of 40 nm showed an increase of 0.6% in the c-lattice parameter and at the same time, related to surface defects, displayed a much smaller lattice expansion than the Zn bulk in the same crystal direction. This has been explained by the fast disappearance of the surface defects, for instance the vacancies, during the heating. Independently whether the explanations given by Wang et al. [32] can be also applied in the present case, it is interesting to remark that both systems show the coincident 'rare' trend to decrease the lattice expansion coefficients with decreasing the crystal size, the origin of which deserves to be investigated in more detail.

Figure 5 shows the TGA and DTA curves obtained for the UO_2 nanoparticles. It is seen that a first weight loss of about 4%, occurs below 200 °C, which can be assigned to physisorbed water. A second weight loss of about 3% follows and takes place below 400 °C, which can be related to chemisorbed water. This coincides with the endothermic peak seen in the DTA curve. The weight loss is complete at around 500 °C. There are some similarities between the TGA curve and the mean strain evolution displayed in Fig. 3, which could indicate that the strain present in the material is due to adsorbed water molecules, exerting a strong influence on the evolution of the crystallite size and the lattice parameter of the UO_2 nanoparticles. It is believed that these molecules of water are present as a hydrated layer around the crystallites. The presence of this layer would lower the effect of the temperature on the crystallite size growth. Indeed while below 700 °C, the crystallite size evolution is slow, i.e., from 3 nm to only about 10 nm, when the strain is then completely released, and likely the water molecules removed, sintering of the nanocrystallites is starting.

Conclusion

Nanocrystallites of UO_2 with a size of 3–5 nm have been studied in situ with HT-XRD and by TGA–DTA. We followed the effect of the temperature on the crystallite size, the lattice parameter, and the strain present in the material. We observed a strong lattice expansion with the crystallite size increase up to 10 nm, where the lattice strain is completely released, the stoichiometry is reduced to UO_2 and the adsorbed water molecules to the compound fully removed. In situ HT-XRD showed that crystallite size and strain in the material are strongly correlated. Indeed below a size of 10–20 nm, the strain is very important while above that size at about 700 °C the strain becomes weak and a stronger effect of the temperature on the crystallite size takes place. Further studies are planned, to follow these effects by transmission electronic microscopy and to investigate the effect of the initial water content on the crystallite size and on the lattice parameter.

Acknowledgements We are grateful to H. Hein for his technical support with TGA–DTA measurements. R. Jovani Abril acknowledges the European Commission for support in the frame of the program "Training and Mobility of Researchers."

References

1. Lai SL, Guo JY, Petrova V, Ramanath G, Allen LH (1996) Phys Rev Lett 77:99
2. Muccillo ENS, Rocha RA, Tadokoro SK, Rey JFQ, Muccillo R, Steil MC (2004) J Electroceram 13:609
3. Ayyub P, Palkar VR, Chattopadhyay S, Multani M (1995) Phys Rev B 51:6135
4. Moon KS, Dong H, Maric R, Pothukuchi S, Hunt A, Li Y, Wong CP (2005) J Electron Mater 34:168
5. Boswell FWC (1951) Proc Phys Soc A 64:465
6. Fukuhara M (2003) Phys Lett A 313:427
7. Qi WH, Wang MP, Su YC (2002) J Mater Sci Lett 21:877
8. Deshpande S, Patil S, Kuchibhatla SVNT, Seal S (2005) Appl Phys Lett 87:133113
9. Fievet F, Germi P, De Bergevin F, Figlarz M (1979) J Appl Cryst 12:387
10. Li G, Boerico-Goates J, Woodfield BF (2004) Appl Phys Lett 85:2059
11. Cimino A, Porta P, Valigi M (1965) J Am Ceram Soc 49:152
12. Solliard C, Fludi M (1985) Surf Sci 156:487
13. Vermaak JS, Kuhlmann-Wilsdorf D (1968) J Phys Chem 72:4150
14. Wasserman HJ, Vermaak JS (1972) Surf Sci 32:168
15. Sun CQ (1999) J Phys 11:4801
16. Wei Z, Xia T, Ma J, Feng W, Dai J, Wang Q, Yan P (2007) Mater Charact 58:1019

17. Li G, Li L, Boerico-Goates J, Woodfield BF (2005) J Am Chem Soc 127:8659
18. Rousseau G, Fattahi M, Grambow B, Desgranges L, Boucher F, Ouvrard G, Millot N, Niepce JC (2009) J Solid State Chem 182:2591
19. Kim HS, Park CH, Park CJ, Choi CB, Jung SH, Suk HC (1994) J Korean Nucl Soc 26:190
20. Amaya M, Nakamura J, Fuketa T (2008) J Nucl Sci Technol 45:244
21. Santa Cruz H, Spino J, Grathwohl G (2008) J Eur Ceram Soc 28:1783
22. Cullity BD (1978) In: Elements of X-ray diffraction, 2nd edn. Addison Wesley, Reading
23. Gronvold F (1955) J Inorg Nucl Chem 1:357
24. Nickel H (1966) Nucleonik 8:366
25. Martin DG (1988) J Nucl Mater 152:94
26. Kittel C (1996) Introduction to solid state physics. Wiley, New York
27. Sui ML, Lui K (1995) Nanostruct Mater 6:651
28. Wagner M (1992) Phys Rev B 45:635
29. Klam HJ, Hahn H, Gleiter H (1987) Acta Metall 35:2101
30. Banerjee R, Sperling EA, Thompson GB, Fraser HL (2003) Appl Phys Lett 82:4250
31. Zhao YH, Sheng HW, Lu K (2001) Acta Metall 49:365
32. Wang Y, Zhao H, Yihua Hu, Ye C, Zhang L (2007) J Cryst Growth 305:8